Are adaptive wavelet discretizations dissipative?

Applications to inviscid Burgers and incompressible Euler equations

Kai Schneider

I2M, Aix-Marseille Université, France

in collaboration with

Rodrigo Pereira[1], Natasha Nguyen van yen[2], Marie Farge[3]

[1]Instituto de Fisica, Universidade Federal Fluminense, Niteroi, Brazil,

[2]FU Berlin, Germany, [3]ENS Paris, France,

5ème Colloque de la Prospective de la FR-FCM

May 19 -20, 2022, Montauban, France

Motivation (physics)

Dissipation models in collisional plasmas and viscous fluids.

In kinetic theory we have the Boltzmann equation:

$$\partial_t f + \mathbf{v} \cdot \nabla_{\mathbf{x}} f + \frac{\mathbf{F}}{m} \cdot \nabla_{\mathbf{v}} f = C(f)$$

In fluid theory we have the Navier-Stokes equation:

$$\begin{cases} \partial_t \mathbf{u} + (\mathbf{u} \cdot \nabla)\mathbf{u} + \frac{1}{\rho}\nabla p = \nu \Delta \mathbf{u} \\ \nabla \cdot \mathbf{u} = 0 \end{cases}$$

pressure

Here we are interested in the vanishing viscosity, vanishing collisionality limit using numerical simulation.

Recent work using MHD, R. Chahine, KS, W. Bos. The effect of shaping on turbulent dynamics in RFP simulations. *J. Plasma Phys.*, 87(6), 2021 and Lagrangian transport in Hasegawa-Wakatani: arXiv.2205.07135

Motivation (maths)

Numerical methods for nonlinear PDEs.

Adaptive Galerkin discretizations have attractive features, e.g. automatic error control using wavelet schemes.

Aim here: use space adaptivity to introduce dissipation.

Give mathematical framework and analyze dynamical Galerkin schemes.

Introduce wavelet based regularization of hyperbolic conservation laws thanks to adaptivity.

Numerical examples for inviscid Burgers (1D) and incompressible Euler (2D and 3D).

Ref.: R. Pereira, N. Nguyen van yen, K. Schneider and M. Farge,
Adaptive solution of initial value problems by a dynamical Galerkin scheme,
SIAM Multiscale Model. Sim., in press, *arXiv:2111.04863*

1. Dynamical Galerkin schemes (1)

2.1. Formal definition. Let H be a Banach space, and consider the equation

$$u' = f(u) \tag{2.1}$$

where u' denotes the weak time derivative of u, where f is defined and continuous from some sub-Banach space $D(f) \subset H$ into H.

Below we shall focus on the case of the 1D Burgers equation on the torus $\mathbb{T} = \mathbb{R}/\mathbb{Z}$:

$$\partial_t u + u\partial_x u = \nu\partial_{xx} u \tag{2.2}$$

which corresponds to (2.1) with

$$f(u) = \nu\partial_{xx} u - u\partial_x u \tag{2.3}$$

The classical Galerkin discretization of (2.1) is defined as follows: for $h > 0$, let H_h be a fixed finite dimensional subspace of $D(f)$, such that:

$$\overline{\bigcup_{h>0} H_h} = H$$

where the adherence is taken in H, and let P_h be the orthogonal projector on H_h.

1. Dynamical Galerkin schemes (2)

To derive this equation, we start with $u_h(t) \in H_h(t)$ for every t, which is equivalent to

$$P_h(t)u_h(t) = u_h(t). \tag{2.6}$$

Differentiating in time leads to:

$$P_h(t)u_h'(t) + P_h'(t)u_h = u_h'(t) \tag{2.7}$$

or equivalently

$$(1 - P_h(t))u_h'(t) = P_h'(t)u_h \tag{2.8}$$

which is the equation we were looking for. By adding (2.5) and (2.8) together, we obtain the definition of the dynamical Galerkin scheme:

$$u_h'(t) = P_h(t)f(u_h(t)) + \underline{P_h'(t)u_h(t)} \tag{2.9}$$

By comparing this differential equation with (2.4), we observe the appearance of a new term proportionnal to the time-derivative of P_h. This is the essential ingredient which characterizes the dynamical Galerkin scheme.

1. Dynamical Galerkin schemes (3)

The above computations are valid when P_h is differentiable, which is a severe restriction and forbids us in particular to switch on and off dynamically some functions in the basis of integration. To pursue we therefore need to extend the definition of the scheme to non-differentiable P_h. For this we consider the integral formulation of (2.9), namely

$$u_h(t) = u_h(0) + \int_0^t P_h(\tau) f(u_h(\tau)) \mathrm{d}\tau + \int_0^t P_h'(\tau) u_h(\tau) \mathrm{d}\tau. \tag{2.13}$$

This equation can be rewritten using a Stieltjes integral with respect to P_h:

$$u_h(t) = u_h(0) + \int_0^t P_h(\tau) f(u_h(\tau)) \mathrm{d}\tau + \int_0^t \mathrm{d}P_h(\tau) u_h(\tau) \tag{2.14}$$

which we call the integral formulation of the dynamical Galerkin scheme.

This equation makes sense as soon as P_h has bounded variation, which gives it a much wider range of applicability than (2.9), allowing in particular discontinuities in P_h. To solve such an equation we need to resort to the theory of generalized ordinary differential equations.

1. Dynamical Galerkin schemes (4)

2.2. Existence and uniqueness of a solution to the projected equations. The rigorous setting for integral equations such as (2.14) involving Stieltjes integrals is explained in detail in the book [9]. An alternative introduction can be found in [3]. We summarize the main consequences of the theory for our problem in the following

THEOREM 2.2. *Assume that $P_h(t) : [0,T] \to$ is BV and left-continuous, that $P_h(0)u_h(0) = u_h(0)$ (i.e. $u_h(0) \in H_h(0)$), and that $f : H_h^0 \to H$ is locally Lipschitz. Then*

(i) There exists T^*, $0 < T^* \leq T$, such that the integral equation

$$u_h(t) = u_h(0) + \int_0^t P_h(\tau)f(u_h(\tau))\mathrm{d}\tau + \int_0^t \mathrm{d}P_h(\tau)u_h(\tau) \tag{2.15}$$

has a unique BV, left-continuous solution $u_h : [0,T^*] \to H_h^0$.

(ii) This solution satisfies

$$\forall t \in [0,T], P_h(t)u_h(t) = u_h(t) \tag{2.16}$$

1. Dynamical Galerkin schemes (5)

(iii) u_h *is continuous at any point of continuity of* P_h*, and more generally for any* t*:*

$$u_h(t^+) - u_h(t) = (P_h(t^+) - P_h(t))u_h(t) \tag{2.17}$$

or equivalently

$$u_h(t^+) = P_h(t^+)u_h(t) \tag{2.18}$$

(iv) *The energy equation (2.10) for smooth* P_h *is replaced in general by:*

$$\frac{1}{2}(\|u_h(t)\|^2 - \|u_h(0)\|^2) = \int_0^t (u_h(\tau), f(u_h(\tau)))\mathrm{d}\tau - \frac{1}{2}\sum_{\{i|t_i<t\}} \|(1 - P_h(t_i^+))u_h(t_i)\|^2, \tag{2.19}$$

where $(t_i)_{i\in\mathbb{N}}$ *are the points of discontinuity of* P_h*.*

Proof: Schauder-Tichonov fixed point theorem and theorems from ref.

[9] S. Schwabik. Generalized ODEs. World Scientific, 1992.

2. Wavelet representation

$$_{ji}(x) = 2^{j/2}\psi(2^j x - i)$$

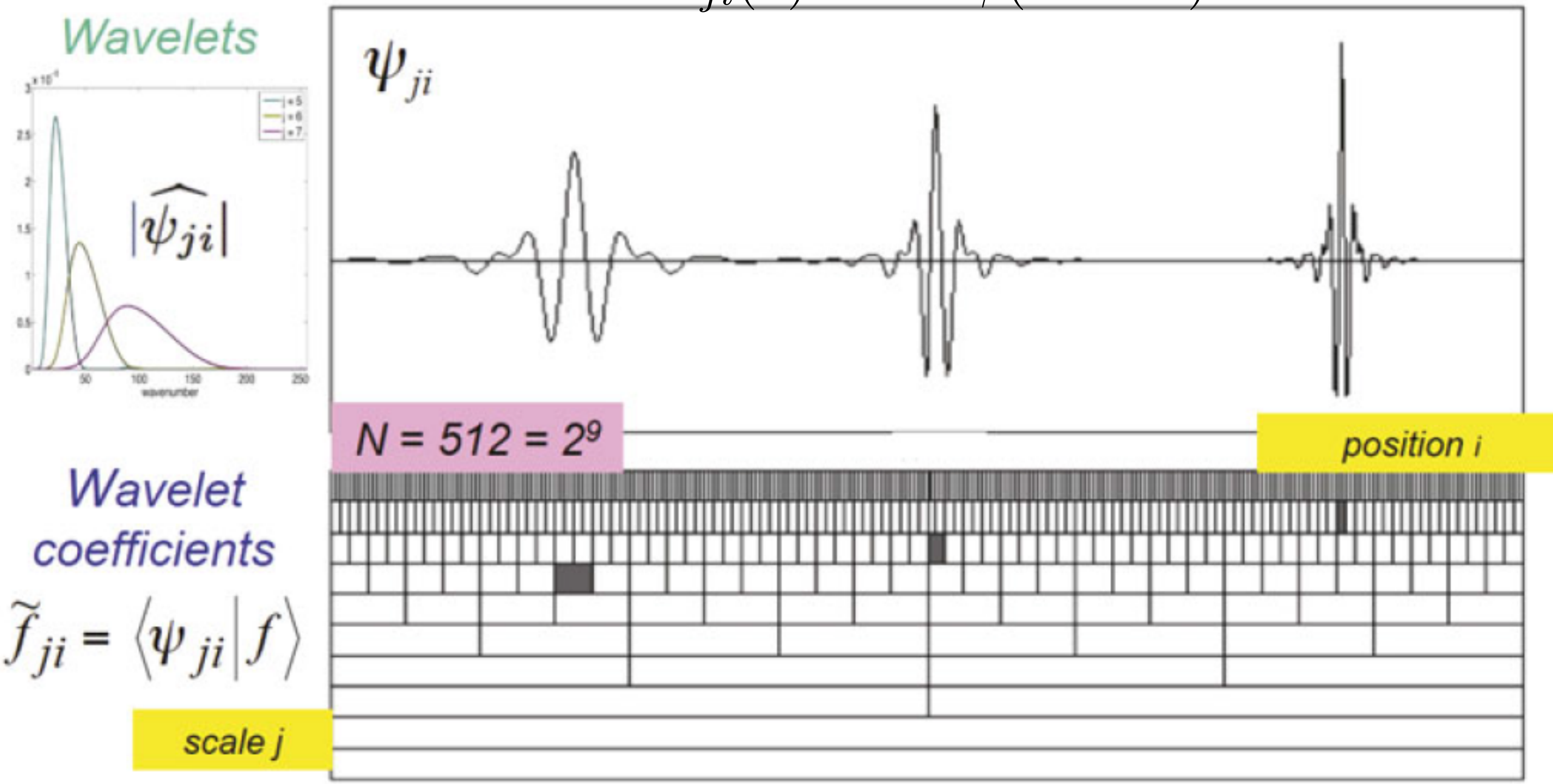

FIGURE 2. Space-scale representation of an orthogonal spline wavelet at three different scales and positions, i.e. $\psi_{6,6}$, $\psi_{7,32}$, $\psi_{8,108}$. The modulus of the Fourier transform of three corresponding wavelets is shown in the inset (top, left).

Inviscid Burgers

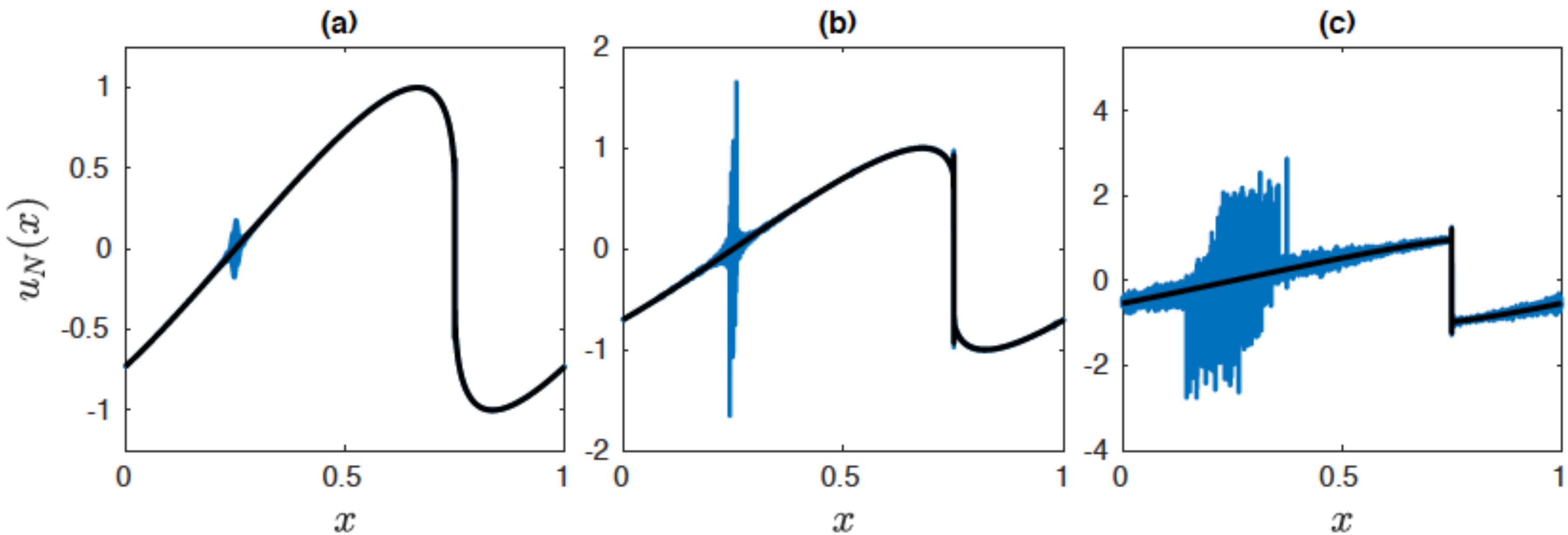

FIG. 5. *CVS-filtered Galerkin truncated inviscid Burgers equation using complex-valued wavelets (Kingslets, in black) together with the non-dissipative Galerkin truncated solution (blue) at times* $t = 0.1644, 0.1793$ *and* 0.3. *The solutions are periodically shifted to the right, so that both the resonances and the shocks can be easily seen.*

$$\partial_t u + \frac{1}{2}\partial_x u^2 = 0 \quad \text{for} \quad x \in \mathbb{T} \quad \text{and} \quad t > 0$$

N.B.: Galerkin truncated Burgers conserves energy and exhibits oscillations (thermal noise due to energy equipartition).

2D incompressible Euler

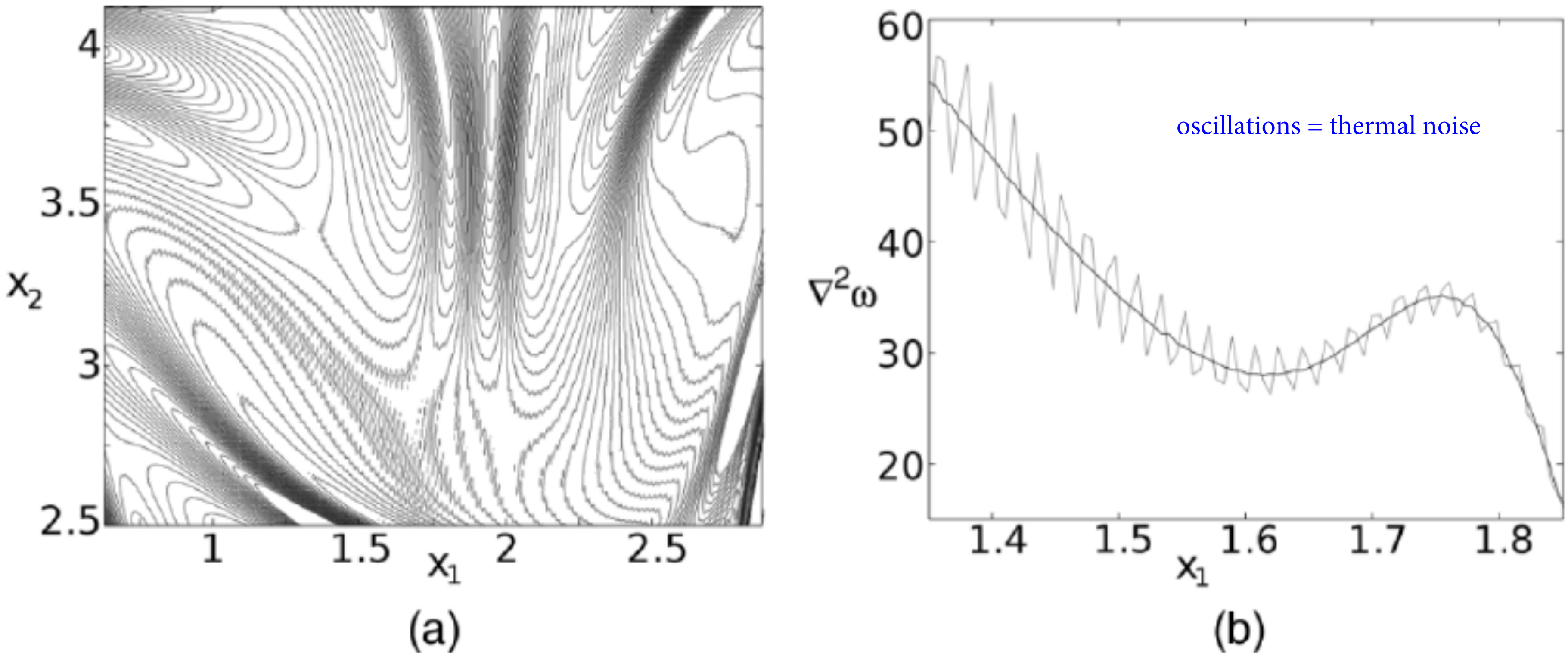

FIG. 8. *Filtering of 2D incompressible Euler using complex-valued wavelets (Kingslets). Left: Contours of the Laplacian of vorticity* $\Delta\omega$ *at* $t = 0.71$. *The Galerkin truncated solution is shown in gray, the CVS solution is given in black. Right: 1D cut of the Laplacian of vorticity for the oscillatory Galerkin truncated solution and the wavelet-filtered smooth solution. From [33].*

$$\partial_t \boldsymbol{u} + (\boldsymbol{u} \cdot \nabla)\, \boldsymbol{u} = -\nabla p \quad \text{for} \quad \boldsymbol{x} \in \mathbb{T}^d \quad \text{and} \quad t > 0$$

$$\nabla \cdot \boldsymbol{u} = 0$$

2D incompressible Euler

Enstrophy

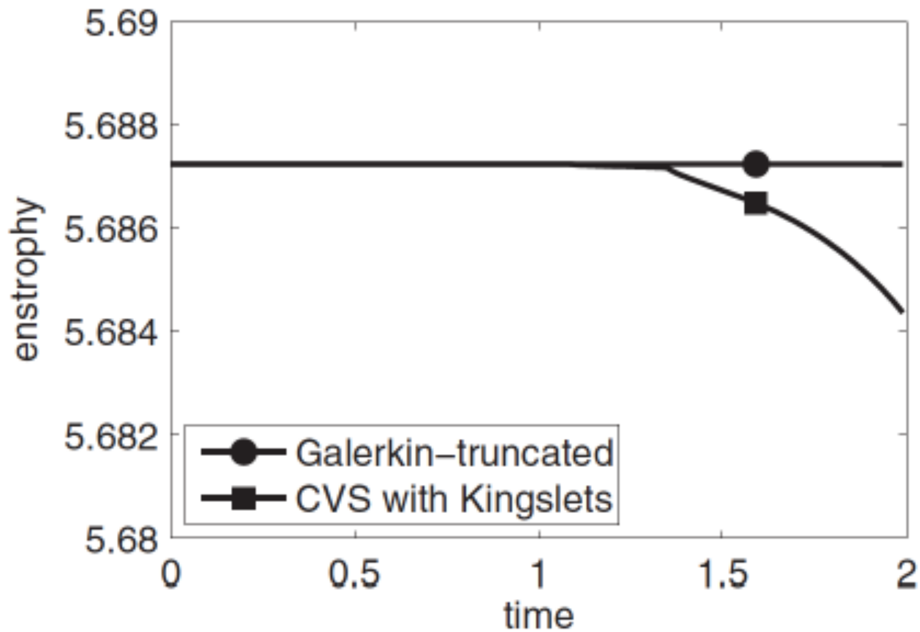

FIG. 9. *Filtering of 2D incompressible Euler using complex-valued wavelets (Kingslets). Evolution of enstrophy* $1/2||\omega||_2^2$ *for the Galerkin truncated case and the adaptive wavelet filtered case using Kingslets. From [33].*

N.B.: Galerkin truncated Euler conserves enstrophy and exhibits oscillations (thermal noise due to enstrophy equipartition).

3D incompressible Euler

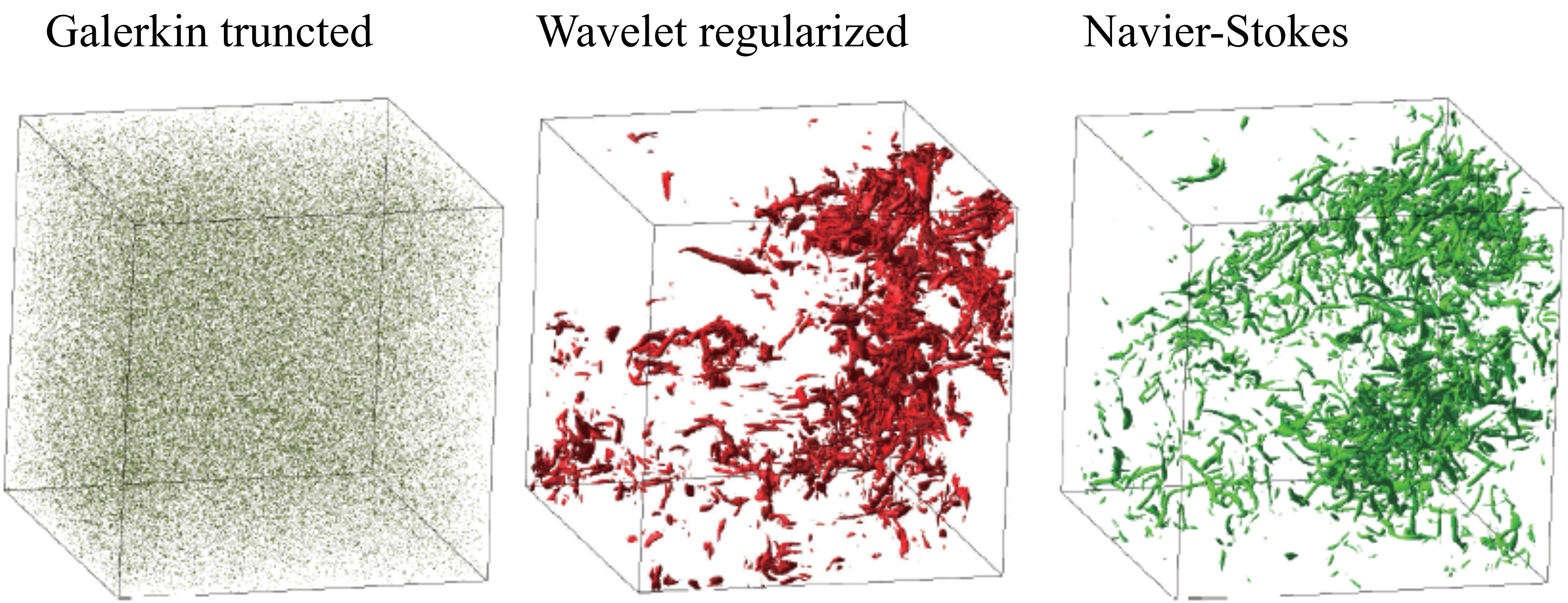

FIG. 11. *Vorticity isosurfaces, $|\boldsymbol{\omega}| = M + 4\sigma$ (where M is the mean value and σ the standard deviation of the modulus of vorticity of NS) for 3D incompressible Euler using Galerkin truncated Euler (Euler, left), wavelet filtered Euler (CVS, center) and Navier-Stokes (NS, right) at time $t/\tau = 3.4$. From [13].*

$$\partial_t \boldsymbol{u} + (\boldsymbol{u} \cdot \nabla)\, \boldsymbol{u} = -\nabla p \quad \text{for} \quad \boldsymbol{x} \in \mathbb{T}^d \quad \text{and} \quad t > 0$$

$$\nabla \cdot \boldsymbol{u} = 0$$

3D incompressible Euler

Energy　　　　　　　　　　　　Enstrophy

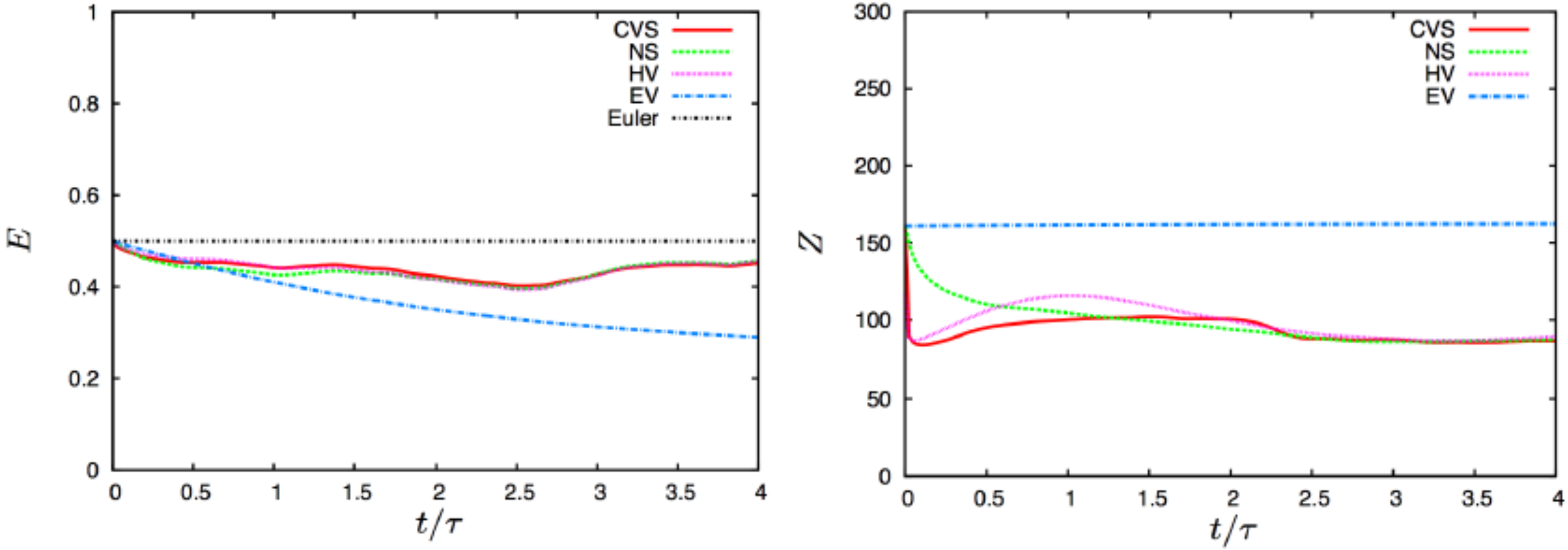

FIG. 10. *Energy (left) and enstrophy (right) evolution for 3D incompressible Euler using for Galerkin truncated Euler (Euler), wavelet filtered Euler (CVS) and Navier-Stokes (NS). HV and EV stand for hyperviscous regularization and EV for Euler-Voigt, respectively, which are not discussed here. From [13].*

N.B.: Galerkin truncated Euler conserves energy and exhibits oscillations (thermal noise due to energy equipartition).

Conclusions

Mathematical framework for analyzing dynamical Galerkin discretizations of evolutionary PDEs.

Nondifferentiable projection operators can introduce energy dissipation.

Mathematical explanation for their regularizing properties due to dissipation.

Adaptivity not only useful to reduce CPU time/memory, but also for introducing dissipation (regularizing effect).

Numerical experiments: 1D Burgers convergence towards the entropy solution. 2D and 3D Euler, thermal noise is removed, but no reference solution is available.

Perspectives are studies of MHD, Hasegawa-Watakani and Vlasov equations using adaptive Galerkin discretizations, in particular wavelet-based schemes and their regularization properties introducing viscous dissipation.

Ref.: R. Pereira, N. Nguyen van yen, K. Schneider and M. Farge,
Adaptive solution of initial value problems by a dynamical Galerkin scheme,
SIAM Multiscale Model. Sim., in press, *arXiv:2111.04863*

Perspectives: FR-FCM in 2022

Multiscale Inertial Particle Transport in the Edge Plasma of tokamaks ('MIPTEP')

High resolution numerical simulations using the Hasegawa-Wakatani model, which governs cross-field transport by electrostatic drift waves in magnetically confined plasmas

Impurity transport both fluid and inertial particles (modeling heavy atoms)

Multiscale statistical analyses of inertial particle distributions

Further develop wavelet-based adaptive proper orthogonal decompositions for reduced order models

Data driven approaches (superresolution using wavelets, CNN for synthesizing artificial particle/impurity distributions)